Acta Neuropathol (2010) 119:135–145
DOI 10.1007/s00401-009-0544-x

CASE REPORT

# Sialidosis type I carrying V217M/G243R mutations in lysosomal sialidase: an autopsy study demonstrating terminal sialic acid in lysosomal lamellar inclusions and cerebellar dysplasia

**Toshiki Uchihara · Ken-ichi Ohashi · Masanobu Kitagawa · Morito Kurata · Ayako Nakamura · Katsuiku Hirokawa · Tsutomu Kasuga · Takayoshi Kobayashi**

Received: 30 January 2009 / Revised: 21 April 2009 / Accepted: 24 April 2009 / Published online: 5 May 2009


**Abstract** Autopsy findings of a patient, with sialidosis type I phenotype carrying V217M/G243R mutations in the lysosomal sialidase gene and biochemically defined isolated sialidase deficiency, who died of intractable lymphoma at the age of 32 years, are described. Perikaryal expansion of cytoplasm was evident, mostly in motor neurons (in the anterior horn and the brain stem), dorsal root ganglia, cerebellar dentate neurons and some neurons in the thalamus and nucleus basalis of Meynert. The stored material was lamellar in lysosomes and exhibited a specific affinity to wheat germ agglutinin at light and electron microscopy, which indicates the accumulation of terminal sialic acid at the non-reducing end of the sugar chain in this pathological structure. Neuronal loss in these nuclei, however, was not frequent in spite of frequent and massive cytoplasmic expansion. Neocortex exhibited a mild spongiosis with some swelling of neurons, which contained lipofuscin-like granules and small amount of lamellar structures in lysosomes. This contrast suggests a discrepancy between the storage process and vulnerability of neurons, both variable according to areas examined. In the cerebellar vermis, dysplastic features, such as abnormal layering of Purkinje cells, thinning and rarefaction of the granule cell layer, incomplete formation of synapse and disordered proliferation of Bergmann's glia, were focally accentuated, suggesting some developmental abnormality not secondary to the storage process. This is the first autopsy demonstration of sialic acid in the lamellar materials and of a developmental abnormality in isolated sialidase deficiency. Additional studies are needed to clarify how this molecular abnormality leads to these morphological and clinical manifestations.

**Keywords** Sialidosis · Autopsy · Lamellar structure · Lectin · Lymphoma · Electron microscopy · Developmental abnormality

T. Uchihara (✉) · A. Nakamura
Department of Neurology, Tokyo Metropolitan Institute for Neuroscience, 2-6 Musashi-dai, Fuchu, Tokyo 183-8526, Japan
e-mail: uchihara-ts@igakuken.or.jp

K. Ohashi · M. Kitagawa · M. Kurata · K. Hirokawa · T. Kasuga
Department of Pathology, Nakano General Hospital, Tokyo, Japan

K. Ohashi
Department of Pathology, Toranomon Hospital, Tokyo, Japan

M. Kitagawa · M. Kurata · K. Hirokawa
Department of Pathology, Tokyo Medical and Dental University, Tokyo, Japan

T. Kobayashi
Department of Neurology, Nakano General Hospital, Tokyo, Japan

## Introduction

Sialidosis is biochemically characterized by a decreased activity in lysosomal sialidase (α-neuraminidase), which cleaves terminal sialic acid of oligosaccharide chain. Molecular bases for this condition are multiple and include (1) "isolated sialidase deficiency", primary deficiency of the enzyme [29] linked to pathological mutations of the gene coding for the lysosomal neuraminidase [3, 16, 23], or (2) "galactosialidosis", a deficit of the protective protein/cathepsin A (PPCA) [5], necessary for proper sorting of the sialidase and β-galactosidase to lysosome and their protection from lysosomal proteolysis. Clinical features of

these two distinct metabolic deficits, however, are shared between each other and their phenotypes have been classified into sialidosis type I and type II [14]. Those with macular cherry-red spot, myoclonus, seizure, ataxia without dementia or skeletal abnormalities have been classified as normosomatic form (sialidosis type I) [8, 21, 24]. Those with dementia and skeletal abnormalities are usually of earlier onset and have been classified as dysmorphic form (sialidosis type II), previously noted as mucolipidosis I [27]. The literature has been greatly confounded because of the similarity of the phenotype of isolated sialidase deficiency and that of galactosialidosis. It is now considered that sialidosis type I phenotype is mostly related to the isolated sialidase deficiency [3, 16, 23], while sialidosis type II phenotype is mostly related to "galactosialidosis" [29]. Here, we report autopsy findings of a sialidosis type I patient with genetically and biochemically defined isolated deficiency of the lysosomal sialidase with retained activity of β-galactosidase. Lectin histochemistry electron microscopy was successful in clarifying that the stored material as lamellar structures contained terminal sialic acid. Moreover, cerebellar dysplasia suggests developmental anomaly possibly related to overrepresentation of sialic acid during development.

## Clinical course

The parents of the patient were born in Ryukyu Islands in the south-west of Japan but were from unrelated families. They have been in good health without motor disturbance or visual impairment, but activity of sialidase in their white blood cells was reported to be moderately decreased. The patient's elder and younger sisters were diagnosed as having cherry red spot-myoclonus syndrome based on ataxic gait, visual impairment, and generalized myoclonic fits that started around the age of 15 years. This diagnosis was confirmed by a marked reduction of sialidase activity in the white blood cells.

The patient was born at nine months of gestation with the birth weight of 2,200 g. The patient had not been aware of his deficits until the age of 15 years, when cherry-red spot was incidentally identified during funduscopic examination. He was referred to a university hospital, where a decreased activity in sialidase was identified, while visual acuity, computed tomography of the brain, and electroencephalogram were normal. At the age of 17 years, he noticed unsteady gait in descending the stairs. At the age of 19 years, generalized seizure developed while playing basketball. Thereafter, his gait disturbance got worse gradually.

On admission to another university hospital at the age of 22 years, cherry-red spot and opacity in the lens were found. General physical examination was otherwise normal. He was fully conscious, but his intelligence was subnormal (verbal IQ; 89, performance IQ; 80, total IQ; 82 on Wechsler Adult Intelligence Scale). Extraocular movements were normal in range and directions except gaze nystagmus. Muscles in the extremities were generally hypotonic, but their strength was normal without atrophy or fasciculations. Myoclonus was elicited on movements, especially when guided by visual information, as we described previously. Myoclonus was not evident when similar movements were performed with his eyes closed [17]. Gait and limb ataxia was present, but it was also possible to interpret this ataxic feature as a manifestation of myoclonic activity induced by movements. Deep tendon reflexes were normal without laterality. No pathological reflexes were elicited. Sensory and autonomic systems were normal. Peripheral blood contained mononuclear cells with multiple vacuoles. Skeletal survey disclosed a deformity in the cervical and lumbar spine. Abdominal ultrasound echography demonstrated mild splenomegaly. Repeated needle electromyography was normal. Giant SEPs were observed by the stimulations of both upper limbs. Activity of sialidase in the peripheral leukocytes was decreased (0.13 nmol/mg protein/h, normal 0.17–2.73) while that of β-galactosidase was within normal range (126 nmol/mg protein/h, normal 71–149). Sequencing of the lysosomal sialidase gene disclosed missense mutations in both alleles; $^{649}$G to A (V217M) and $^{727}$G to A (G243R) [20]. At the age of 30 years, a nontender nodule was noted in the right axilla. The biopsied nodule disclosed malignant lymphoma of diffuse large B cell type (stage IIIA), which was refractory to multiple courses of standard (CHOP) and intensified (ESHAP) chemotherapy and to local irradiation for palliation. Terminal course was complicated by profound pancytopenia, anemia, liver dysfunction, ascites, and pleural effusion and the immediate cause of death was respiratory failure.

## Materials and methods

The brain and the spinal cord were fixed in 10% buffered formalin for 3 weeks. Cerebral hemispheres were sliced along the coronal plane and the brainstem was sliced perpendicular to the long axis. They were embedded in paraffin wax. Deparaffinized sections were subjected to routine histological stains (H&E, Klüver–Barrera and Bodian stains) and Masson–Fontana stain for lipofuscin. They were subjected to immunohistochemistry with the standard avidin biotin-peroxidase method using primary antibodies listed in Table 1. Small pieces of the spinal cord and dorsal root ganglia (DRG) were similarly fixed in formalin, cryoprotected with 20% sucrose and free-floating

**Table 1** Primary antibodies used in this study

| Epitope | ID | Species/class | Dilution | Source |
|---|---|---|---|---|
| Neurofilament | SMI31 | Mouse IgG | 1:10,000 | Sternberger–Meyer |
| Neurofilament[a] | SMI32 | Mouse IgG | 1:1,000 | Covance |
| αB-crystallin[a] | G2JF | Mouse IgG | 1:3,000 | NovoCastra |
| MAP2[a] | HM-2 | Mouse IgG | 1:1,000 | Sigma |
| Calbindin[b] | Kj6 | Mouse IgG | 1:200 | NovoCastra |
| NeuN[a] | MAB377 | Mouse IgG | 1:3,000 | Chemicon |
| SNAP25 | SMI81 | Mouse IgG | 1:10,000 | Sternberger–Meyer |
| GFAP | Z334 | Rabbit IgG | 1:1,000 | DAKO |
| Ubiquitin | Z0458 | Rabbit IgG | 1:1,000 | DAKO |
| PHF-tau (AT8) | BR3 | Mouse IgG | 1:10,000 | Innogenetics |
| α-Synuclein[c] | PSyn#64 | Mouse IgG | 1:10,000 | WAKO |

[a] Heating with autoclave

[b] Heating with microwave

[c] Formic acid (5 min at room temperature) is necessary as pretreatment

sections were obtained. Free floating sections were subjected to histochemical staining with alcian blue, periodic acid Schiff or lectin probes for light, and electron microscopy. Pieces of formalin fixed tissue were postfixed in osmium tetroxide and embedded in epon. Ultrathin sections were stained with uranyl acetate and lead citrate and were observed under an electron microscope (H-7000, Hitachi, Tokyo, Japan). For lectin histochemistry, free-floating sections were treated with 1% hydrogen peroxide to inactivate endogenous peroxidases. They were then incubated overnight with biotinylated wheat germ agglutinin (WGA, Seikagaku kogyo, Tokyo, Japan) or biotinylated *Ricinus communis* agglutinin (RCA, Seikagaku kogyo). The biotin signal was amplified with ABC method (ABC Elite, Burlingame, CA, USA) and was visualized with diaminobenzidine with nickel ammonium chloride as a chromogen to yield purple precipitates. They were then counterstained with nuclear fast red. Some of the stained sections were postfixed with osmium tetroxide and dehydrated through a series of alcohol and embedded in epon. Ultrathin sections were similarly observed under the electron microscope.

## Results

General autopsy revealed swelling of multiple lymph nodes such as paraaortic, subclavian, peribronchial, perigastric, parapancreatic, and mesenteric nodes, up to walnut size. Hepatosplenomegaly was also obvious weighing 2,250 g for the liver and 790 g for the spleen. Histological examination demonstrated that malignant lymphoma, diffuse large B-cell lymphoma, involved the systemic lymph nodes, liver, spleen, lungs, kidneys, and adrenal glands. Direct cause of death would be respiratory failure caused by severe pulmonary edema and massive pleural effusion due to a remarkable infiltration of malignant lymphoma cells into the lung.

The brain weighed 1,320 g and was unremarkable on macroscopic examination (Fig. 1a) except for mild depigmentation of the substantia nigra and mild atrophy in the cerebellar dentate nucleus (Fig. 1b). Mild spongiosis was found in the superficial layers of cerebral cortices (Fig. 1c). Cytoplasmic expansion was evident in motor neurons (Fig. 2a, in the anterior horn as well as in the brain stem motor nuclei), DRG (Fig. 2b), cerebellar dentate neurons and some neurons in the thalamus and nucleus basalis of Meynert. The expanded perikarya were filled with luxol-fast blue-positive granules (Fig. 2c, Klüver–Barrera staining). Lipofuscin granules were identified in some neurons (arrowheads, Fig. 2d, Masson–Fontana staining, also confirmed with autofluorescence) but they were rare in neurons with cytoplasmic expansion (arrows, Fig. 2d). On floating sections, they were strongly positive for PAS (Fig. 2e) and alcian blue (Fig. 2f). Neuronophagia was infrequent relative to massive and consistent swelling of neurons in these areas (Fig. 2a, arrows). Cytoplasmic swelling was occasionally found in some pyramidal neurons of cerebral cortices (Fig. 1d) and of hippocampus. They sometimes contained granules positive for Masson–Fontana staining. Neuronophagia was rare in these areas. Severity of neuronal loss, gliosis and perikaryal expansion and their regional differences are shown as Table 2.

The expanded cytoplasm of neurons exhibited essentially similar immunohistochemical profiles throughout the brain. In the anterior horn, a neurofilament immunoreactivity (SMI32, Fig. 2g) was observed in some neurons while it was less intense in neurons with cytoplasmic expansion (arrowheads, Fig. 2g). Immunoreactivity for another neurofilament epitope (SMI31) was less intense, especially in neurons with cytoplasmic expansion (arrowheads, Fig. 2h). These neurons were negative for MAP2 (Fig. 2i), αB-crystallin (Fig. 2j), ubiquitin (Fig. 2k), PHF-tau (AT8, data not shown), and α-synuclein (data not shown). Numerous spheroids in the gracilis nuclei were positive for neurofilament epitope SMI31 (Fig. 2l).

Although the cerebellar cortex was macroscopically unremarkable (Fig. 1b), microscopic examination clarified focal disorganization of cerebellar cortex in the vermis. The boundary between the molecular layer and the granule cell layer was obscure, especially in the bottom of some cerebellar folia (Fig. 3a). This was accompanied by focally accentuated thinning and rarefaction of the granule cell layer (black asterisk, Fig. 3a). In contrast with sharp demarcation of cerebellar layers in control (Fig. 3b,

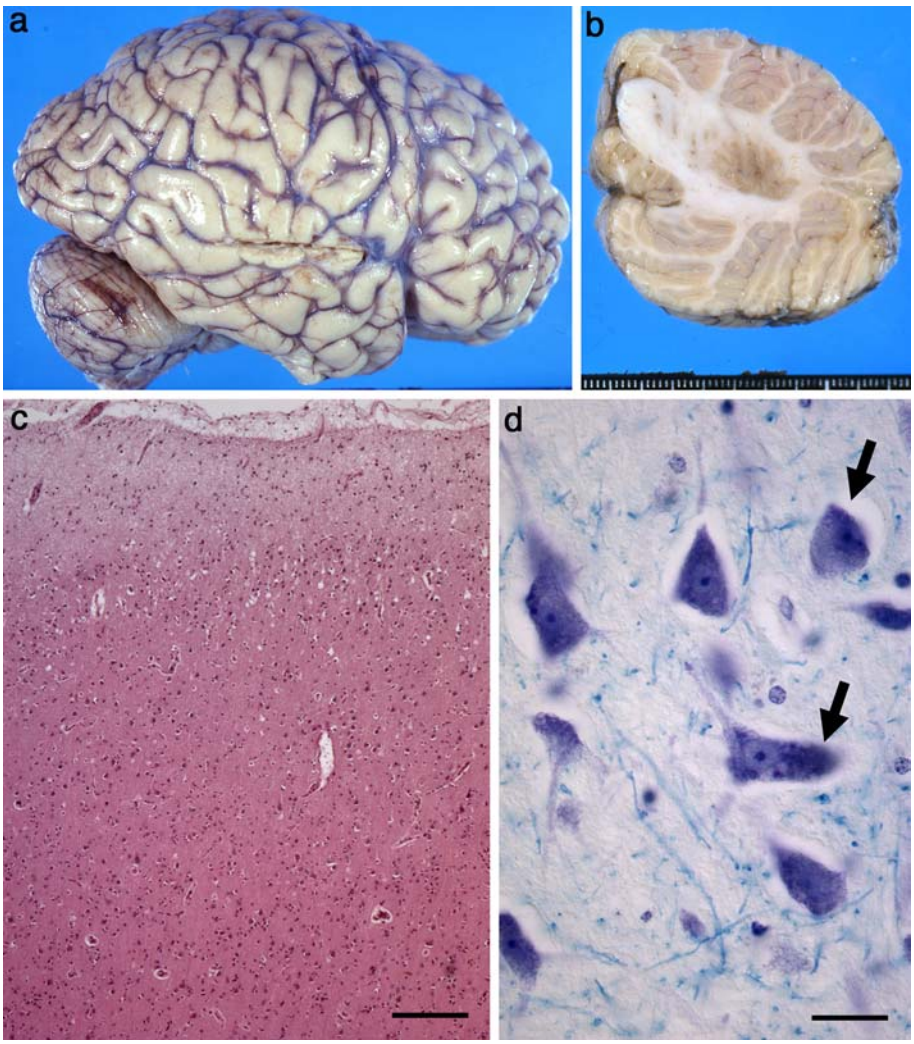


**Fig. 1** Macroscopic and microscopic findings. **a** Right lateral view of the brain without apparent macroscopic abnormalities. **b** Sagittal view of the cerebellar hemisphere with mild atrophy and discoloration of the dentate nucleus. **c** Mild spongiosis in superficial layers of the frontal cortex (H&E, *bar* 200 μm). **d** Pyramidal neurons in the cortex containing luxol fast blue-positive substance (*arrows*, Klüver–Barrera staining, *bar* 25 μm)

synaptic stain with SNAP25), the boundary between the molecular layer and the granule cell layer (white asterisk, Fig. 3c, synaptic stain with SNAP25) was obscured. This was accompanied by an aberrant extension of dense synaptic components of molecular layer into the granule cell layer (black asterisk, Fig. 3c, synaptic stain with SNAP25), where granule cells were focally depleted (black asterisk, Fig. 3d, NeuN immunostain). At a higher magnification of the same area on the neighboring sections, positioning of Purkinje cells (arrowheads, Fig. 3e, calbindin immunostain) were aberrant, not aligned along the boundary between the molecular layer and the granule cell layer (white asterisk). Bergmann glia, usually aligned along this boundary (white asterisk, Fig. 3f, GFAP immunostain), were absent. Instead, GFAP-positive fibers were scattered in the granule cell layer and around the aberrant Purkinje cells (arrowheads, Fig. 3f). The Purkinje cells with swellings in their soma and dendrites were variously positive with Klüver–Barrera (asterisk, Fig. 3g) and PAS stainings. A few large binucleated neurons were found in the Purkinje cell layer (Fig. 3h). In addition, loss of Purkinje cells and proliferation of Bergmann's glia with thinning of molecular layer were noted in inferior aspects of the cerebellar hemisphere. The presence of swollen Purkinje cells has no relation to the loss of Purkinje cells or their abnormal arrangement.

The nature of the material stored in the expanded perikarya was evaluated with lectin histochemistry on floating sections of the spinal cord or of DRG. The expanded perikarya of these neurons was positive for WGA (a ligand for sialic acid or *N*-acetyl neuraminic acid, Fig. 4a) but negative for *R. communis* agglutinin (RCA, a ligand for D-galactose, Fig 4b), suggesting that the terminal sugar moiety of accumulated oligosaccharide chain was *N*-acetyl neuraminic acid (NAcNA = sialic acid) at the non-reducing end. This specific affinity of the WGA lectin to NAcNA was further supported by the disappearance of this labeling either upon coincubation of the biotinylated WGA with NAcNA (Fig. 4c) or after the pretreatment with neuraminidase (Fig. 4d, Roche, 1 U/ml in 0.05 M sodium

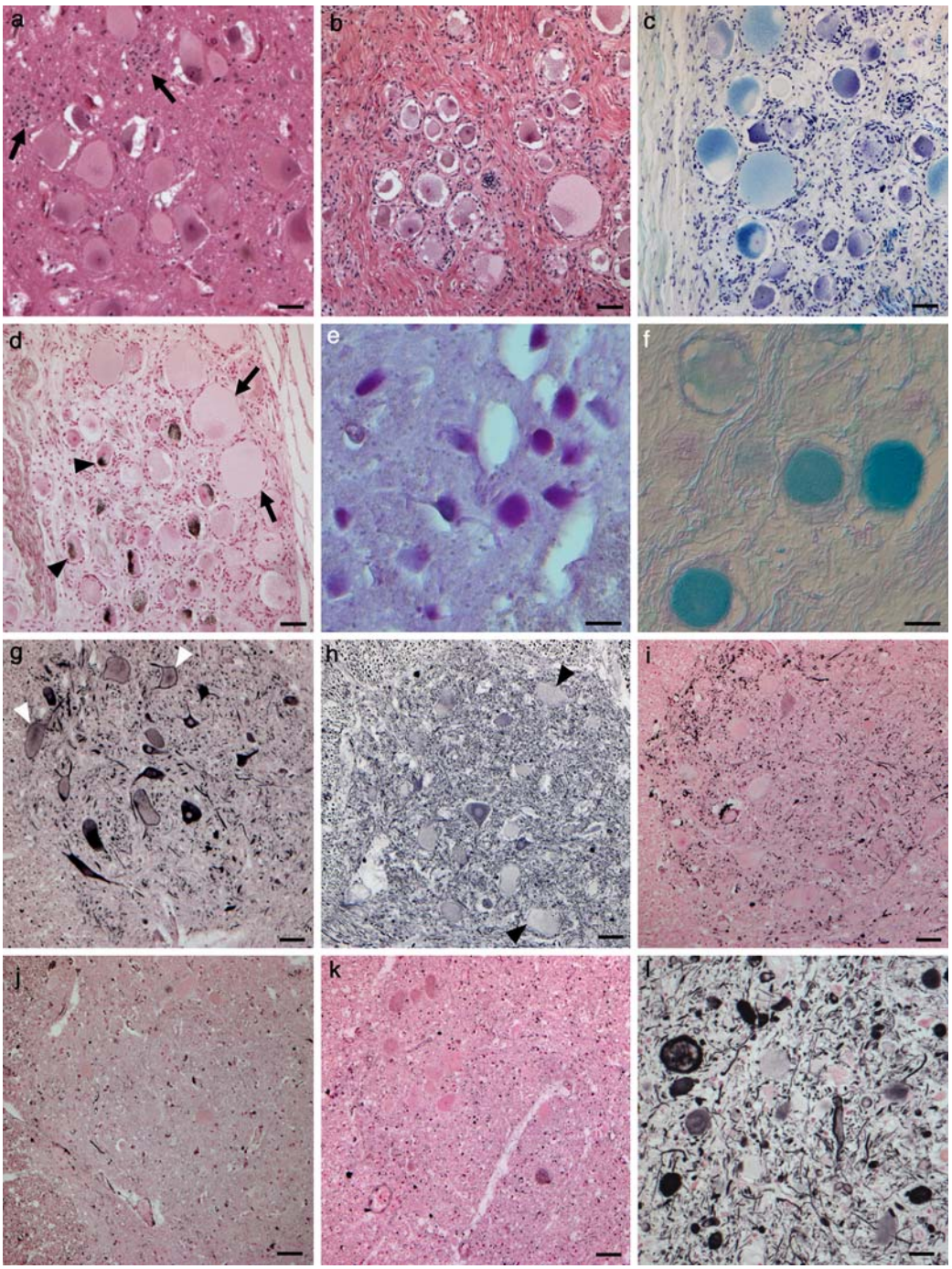


**Fig. 2** Light microscopic findings of neurons with perikaryal expansion. **a** Marked perikaryal expansion of anterior horn cells of the spinal cord. Neuronophagia was infrequent (*arrows*) in spite of frequent and marked expansion of neuronal cytoplasm (H&E), **b** marked perikaryal expansion of the neurons of the dorsal root ganglion (DRG, H&E), **c** perikaryal expansion of DRG neurons was stained with luxol fast blue (Klüver–Barrera staining), **d** accumulation of lipofuscin granules in some DRG neurons (*arrowheads*) but rarely in neurons with perikaryal expansion (*arrows*, Masson–Fontana staining), **e** anterior horn cells of the spinal cord strongly positive for PAS, **f** DRG neurons strongly positive for alcian blue, **g** neurofilament-immunoreactivity (SMI32) in anterior horn cells was variable and less concentrated in neurons with perikaryal expansion (*arrows*), **h** neurofilament-immunoreactivity (SMI31) was weak in anterior horn cells with perikaryal expansion (*arrows*), **i**–**k** no immunoreactivity to MAP2 (**i**), αB-crystallin (**j**) and ubiquitin (**k**) in anterior horn cells, **l** axonal spheroids, with variable SMI31 immunoreactivity, were abundant in the gracilis nucleus. *Bar* 50 μm (**a**–**k**), *bar* 25 μm (**l**)

**Table 2** Regional differences in lesions

| Region | Neuronal loss | Gliosis | Perikaryal expansion |
|---|---|---|---|
| Anterior horn cells | NP | 1 | 3 |
| Dorsal root ganglia | NP | 0 | 3 |
| Posterior column nuclei | NP | 0 | 3 |
| Inferior olives | 0 | 1 | 0 |
| Pontine nuclei | 1 | 2 | 2 |
| Facialis nucleus | 0 | 1 | 0 |
| Spinal trigeminal nucleus | 0 | 1 | 2 |
| Locus ceruleus | 0 | 0 | 3 |
| Ambiguus nucleus | 0 | 0 | 3 |
| Substantia nigra | 0 | 1 | 0 |
| Nucleus ruber | 0 | 0 | 0 |
| Oculomotor nucleus | 0 | 0 | 3 |
| Cerebellar dentate nucleus | 0–1 | 1 | 3 |
| Purkinje cells (cytoplasm) | 0–3 | 0 | 2 |
| Purkinje cells (dendrites) | – | – | 2 |
| Striatal neurons (large) | 0 | 0 | 2 |
| Striatal neurons (small) | 0 | 0 | 0 |
| Globus pallidus | 0 | 1 | 1 |
| Thalamus | 0 | 1 | 3 |
| Nucleus basalis (Meynert) | 0 | 0 | 3 |
| Hyppocampal pyramidal neurons | 0 | 0 | 2 |
| Hyppocampal dentate neurons | 0 | 0 | 0 |
| Betz cells | 0 | 0 | Infrequent |
| Cortical pyramidal neurons | 0–1 | 1 | 1–2 |

*NP* Neuronophagia, *infrequent* only some Betz cells exhibited neuronal swelling, *0* not detectable, *1* mild, *2* moderate, *3* severe, – not applicable

acetate and 1% $CaCl_2$, pH 5.5 at 37 for 20 h) prior to the exposure to biotinylated WGA. This affinity to WGA was observed also in the liver tissue (Fig. 4e). It disappeared similarly upon coincubation with NAcNA (Fig. 4f). This WGA-labeling with confirmed specificity to the terminal sialic acid was unstable with paraffin-embedded specimens or floating sections after harsh lipid extraction procedures such as (1) treatment with alcohol/5% acetic acid or (2) treatment with 8 volume of chloroform/1 volume of diethyl ether/1 volume of 95% ethanol.

Cortical neurons contained lipofuscin granules (Fig. 5a, asterisk) and lamellar structures (Fig. 5a, rectangle). These lamellar structures were contained in vacuoles lined by a unit membrane (Fig. 5b). These vacuoles containing lamellar structures were more abundant in the anterior horn cells in the spinal cord (Fig. 5c) but rarely contained lipofuscin granules. The electron density and the interval of these lamellar structures were heterogeneous (Figs. 5b, d). At the maximum magnification, they were composed of electron-dense bilayer unit with an interval of 4.5 nm (Fig. 5e). This lamellar structure was positive for WGA (Fig. 5f, arrows). Some dendrites in cerebellar Purkinje cells also contained similar lamellar structures. Renal glomeruli and renal tubules also contained vacuoles, but electron dense materials or lamellar structures were absent in these vacuoles (Fig. 5g). Concentric profiles, finger-print patterns, or curvilinear structures were not apparent.

## Discussion

This is a detailed autopsy report on a patient with genetically and biochemically defined isolated sialidase deficiency. Histochemical examinations disclosed that the stored material was rich in a sugar moiety as evidenced by robust staining with PAS (Fig. 2e) and alcian blue (Fig. 2f). Furthermore, we confirmed its specific affinity to WGA, suggesting that the terminal sugar moiety of accumulated oligosaccharide chain was *N*-acetyl neuraminic acid (NAcNA, sialic acid) at the non-reducing terminal. This is compatible with the metabolic disturbance expected from the reduced activity of sialidase, which cleaves terminal sialic acid. Moreover, structures found in the vacuoles were lipofuscin-like granules and lamellar structures, sometimes in the same vacuoles, suggesting that these pathological processes are concerned with the lysosome. To our knowledge, this is the first confirmation in human autopsy samples with the molecular diagnosis of isolated sialidase deficiency that the stored materials in lysosomes of neurons are lamellar in structure. Furthermore, using lectin histochemistry, we successfully demonstrated that these stored materials contain a sugar moiety with terminal sialic acid at the non-reducing end. Lamellar structure has been reported in the spinal cord of a neonatal case with biochemically defined sialidosis [31]. However, these lamellar structures were not evident in Purkinje cell cytoplasm or in neurons of cerebral cortex [31]. Although this is in agreement with our observation, we identified similar lamellar structure in the dendrites of Purkinje cells, which correspond to focal swelling of Purkinje cell dendrites containing PAS-positive materials. Cortical neurons of sialidosis type I had been examined through brain biopsy [7] or autopsy [1] and contained lysosome-related vacuoles. Electron dense materials in these vacuoles in cortical neurons of sialidosis type I, however, had been described as membranovesicular body, compound body, lysosome-like body or lipofuscin [1, 7] and were not lamellar as reported in the renal tubules and glomeruli [31], liver tissue [6, 15, 24] and ganglion cells in the gastrointestinal tract [10]. In our patient, neurons in the cerebral cortex contained not only lipofuscin granules, verified with EM and Masson–Fontana staining, but also small amounts of lamellar structures in lysosomes. Amano et al. [2] reported membrane-bound lamellar structure in the

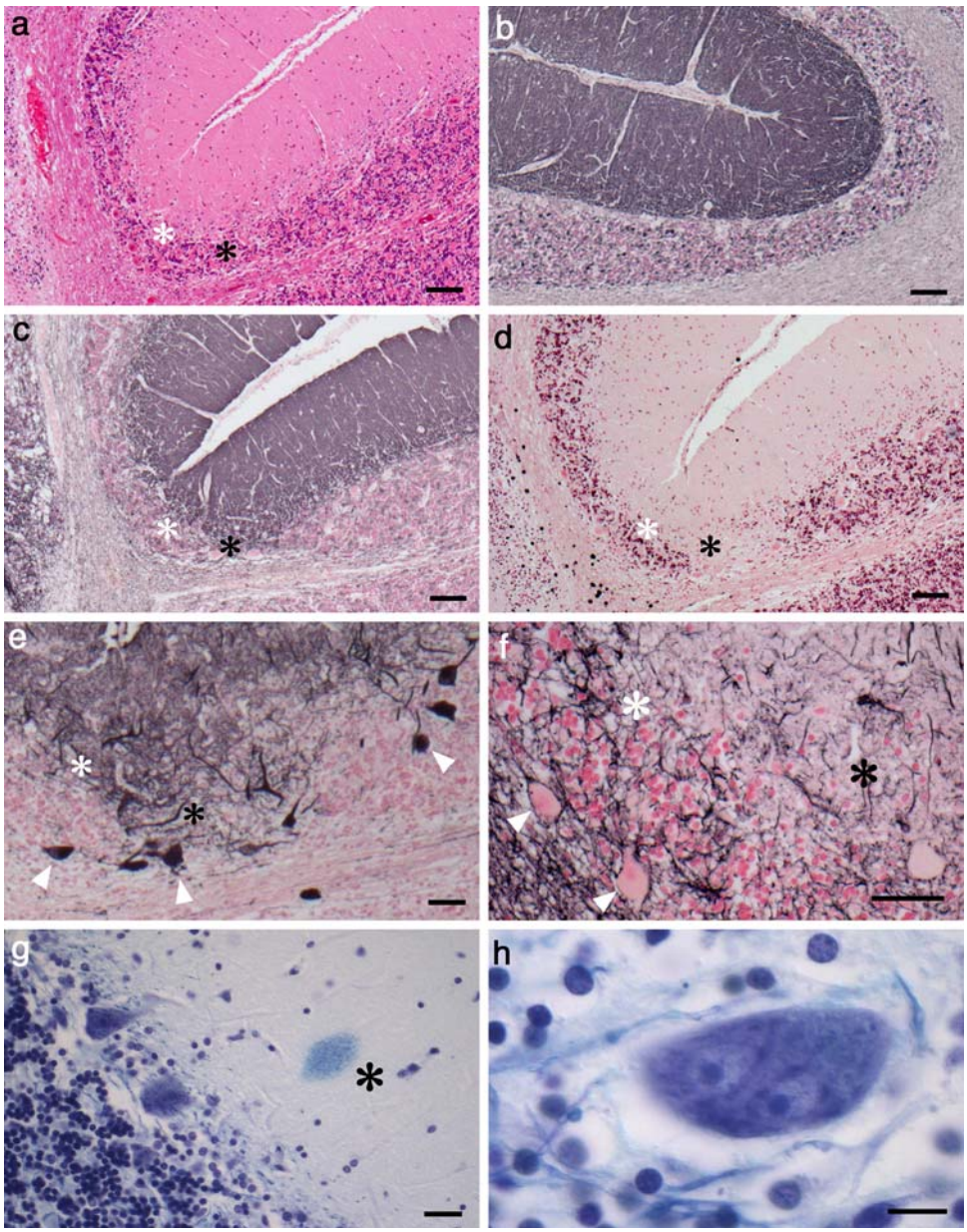


**Fig. 3** Focal dysplasia of cerebellar cortex. **a** The boundary between the molecular layer and the granule cell layer (*white asterisk*) was obscure, especially in the bottom of some cerebellar folia (H&E). Thinning and rarefaction of the granule cell layer was focally accentuated (*black asterisk*), **b** sharp demarcation of cerebellar layers in control (synaptic stain with SNAP25), **c** obscured boundary between the molecular layer and the granule cell layer (*white asterisk*) and aberrant extension of dense synaptic components of molecular layer into the granule cell layer (*black asterisk*, synaptic stain with SNAP25), **d** focally accentuated rarefaction and thinning of granule cells (*black asterisk*, NeuN immunostain), **e** aberrant positioning of Purkinje cells (*arrowheads*, calbindin immunostain), not aligned along the boundary between the molecular layer and the granule cell layer (*white asterisk*). The *black* and *white asterisks* represent same positions throughout **a**, **c**, **d**, **e**, **f** in the neighboring sections, **f** Bergmann glia, usually aligned along the boundary between the molecular and granule cell layers (*white asterisk*), were absent in this area of focal dysplasia. Instead, GFAP-positive fibers were scattered in the granule cell layer and around Purkinje cells (*arrows*, GFAP immunostain), **g** Focal swelling of Purkinje cell dendrite containing luxol fast blue-positive substance (*asterisk*, Klüver–Barrera), **h** A binucleated neuron in the Purkinje cell layer (Klüver–Barrera) *bar* 50 μm (**a**–**d**), *bar* 25 μm (**e**–**g**), *bar* 10 μm (**h**)

anterior horn cells of an autopsy case with galactosialidosis, a similar disorder in which enzyme activity of β-galactosidase is deficient in addition to sialidase deficiency. In contrast, it was interesting to observe that neurons in the cerebral cortex in their patient contained lipofuscin granule but not these lamellar structures [2]. Apparently, the initial biopsy of the cerebral cortex from a patient with sialidosis type I [7] identified just lysosomal contents without lamellar

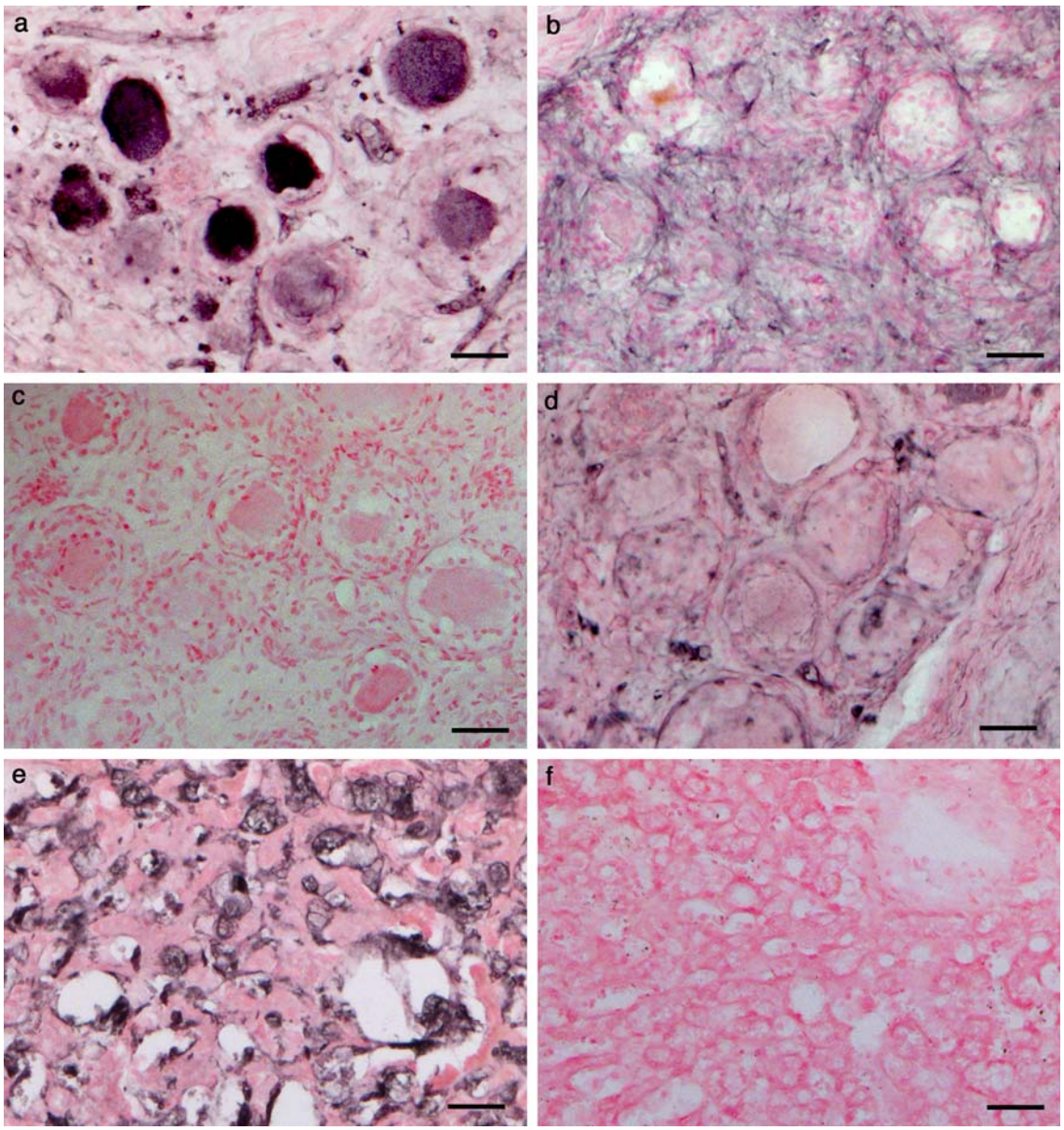


**Fig. 4** Terminal sialic acid with lectin histochemistry. **a** Neurons with perikaryal expansion in DRG were positive for wheat germ agglutinin (WGA), a ligand for terminal sialic acid, **b** they were negative for *Ricinus communis* agglutinin (RCA), a ligand for terminal D-galactose. **c** This reactivity to WGA was abolished when coincubated with *N*-acetyl neuraminic acid; **d** or after pretreatment with sialidase. **e** Liver tissue exhibited a similar affinity to WGA; **f** abolished when coincubated with *N*-acetyl neuraminic acid. Counter stained with nuclear fast red. *Bar* 50 μm (**a**–**f**)

structures, because these lamellar structures, rich in lower motor neurons and DRG, are scarce in the cerebral cortex. Although reports on these storage material in related disorders are still limited [22], it is likely that this regional difference in intralysosomal structures is shared among sialidosis, galactosialidosis and earlier cases when biochemical definition was not yet available [12].

In spite of the storage process, differently represented according to the site affected, neuronal loss was not necessarily correlated with the degree of the storage, as reported previously in these disorders [2, 22]. For example, the neurons in the anterior horn of the spinal cord and in DRG were the examples of marked perikaryal expansion containing the lamellar structures. The number of remaining neurons in these areas was normal with little neuronophagia. Functional integrity of these lower motor neurons even with massive perikaryal expansion with lysosomal storage was further corroborated clinically by the absence of denervation potentials on repeated needle electromyography. On the other hand, mild spongiosis

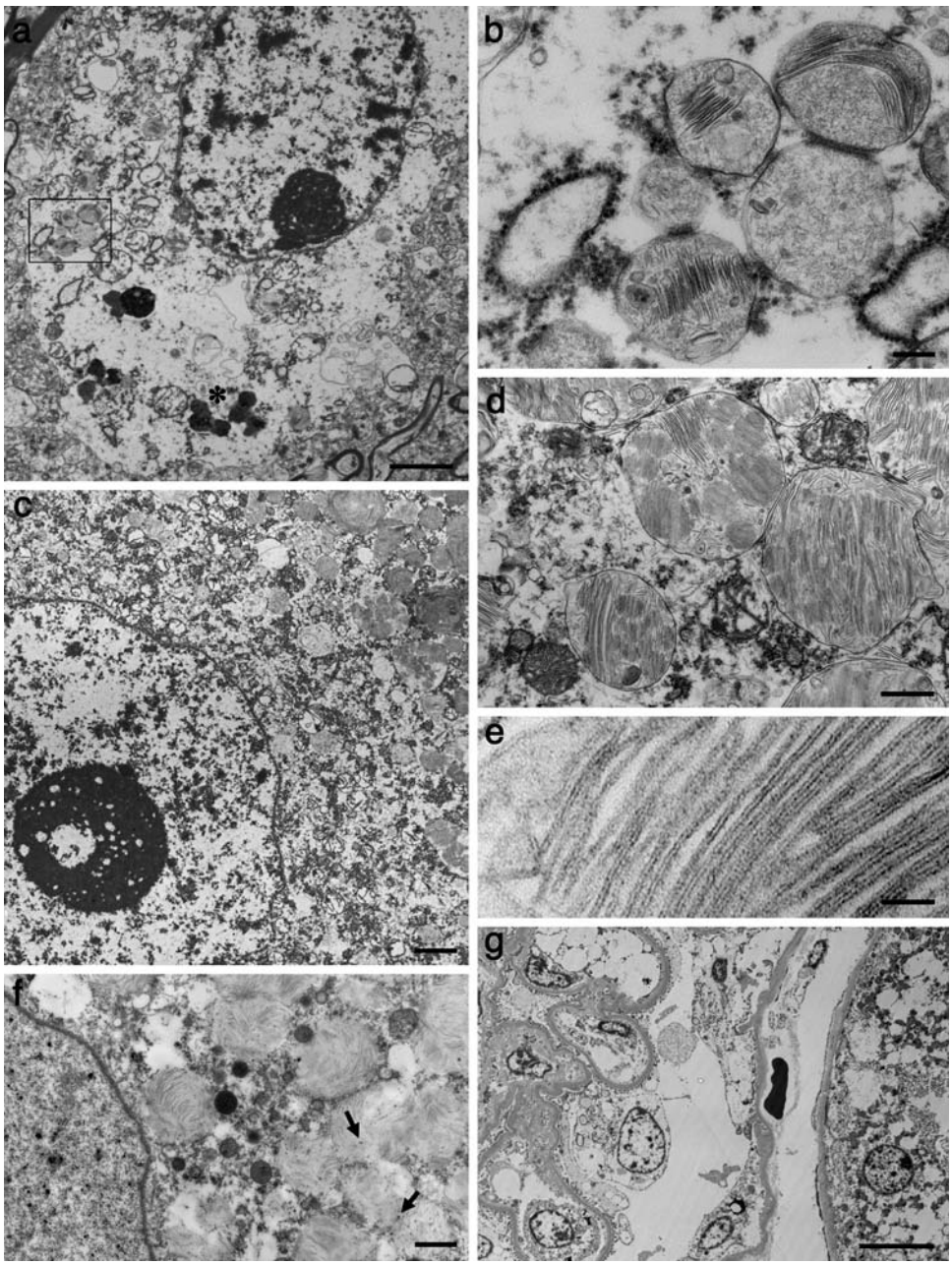


**Fig. 5** Lamellar structures with terminal sialic acid in lysosome. **a** A pyramidal neuron in the cerebral cortex containing lipofuscin granules (*asterisk*) and electron-dense lamellar structures within vacuoles (*rectangle*), *bar* 2μ. **b** High-power view of the *rectangle* in **a**. Lamellar structures were contained in vacuoles lined by a unit membrane. *Bar* 200 nm. **c** An anterior horn cell filled with lamellar structures but lipofuscin granules were extremely rare. *Bar* 2μ. **d** Abundant lamellar structures in the anterior horn cells in the spinal cord. They were contained in vacuoles lined with a unit membrane. *Bar* 500 nm. **e** High-power view of the lamellar structure, which is composed of bilayer of electrondense material with an interval of 4.5 nm. *Bar* 100 nm. **f** Floating section from DRG probed with biotinylated-wheat germ agglutinin (WGA) visualized after avidin-biotin-peroxidase method with diaminobenzidine. The lamellar structures exhibited the reactivity to WGA (*arrows*). *Bar* 1 μm. **g** Kidney. Multiple components of glomerulus (*left*) and of renal tubules (*right*) contained vacuoles but lamellar structures were not evident in these vacuoles. *Bar* 10 μm

was found in the cerebral cortices, where only lipofuscin granules were identified, but the lamellar structures were scarce. Similar regional differences have been described in galactosialidosis [2]. Although the coexistence of lamellar structures and lipofuscin in the same lysosome suggests that these two processes are closely related, we have no clear explanation how these pathological processes are represented differently according to the sites and diseases [13] and how they are related to neuronal death.

Large B-cell type lymphoma of this patient was extremely refractory to chemotherapy and radiation. Association of lymphoma to sialidosis type I has not been described in the literature and could have occurred by chance. However, a series of evidence suggests a possible link between sialidase/sialic acid and malignancy [18]. Indeed, it is interesting that underrepresentation of sialidase in some cell lines of colon carcinoma is related to their highly metastatic nature relative to cell lines expressing more abundant sialidase [26]. This hypothesis is in agreement with an observation that the presence of sialic acid on the surface of diffuse large B cell lymphoma is associated with shorter survival [28]. Because overexpression of lysosomal-type sialidase leads to suppression of metastasis of a

melanoma cell line [11], it is highly probable that the pathological mutations of the lysosomal sialidase gene of our patient were related to the extreme aggressiveness of his lymphoma. It is worth noting that siblings of this patient developed colon cancer and ovarian tumor, further corroborating a possible link between sialidase deficiency and neoplasm. At any rate, this intractable lymphoma truncated the life of this patient much earlier than expected from the natural history of sialidosis type I, providing us with an opportunity to examine pathological changes due to the sialidase deficiency, not at the extreme terminal stage of the disease. A possible relation of the storage process to neuronal death is, however, further complicated in the cerebellum, where arrangement of each cell component is focally deranged. This focally accentuated dysplastic nature affecting Purkinje cells, granule cells, synapses and Bergmann's glia is hardly explained by the storage process and cell death. Indeed, expression of sialic acid is regulated in the developing cerebellum [25] and the presence of sialic acid on the neuronal surface is related to neurite growth [4]. Although similar abnormalities have not yet been described so far in this and related diseases, a possible role of sialic acid during morphogenesis of the brain suggests that the inherent metabolic abnormality yielding an excessive amount of sialic acid may lead to disordered structuring of the cerebellar cortex. Because neuronal depletion was accentuated in the lower aspect of cerebellar hemisphere, where neither neuronal swelling nor abnormal arrangement of neurons was accentuated, it is plausible that these three aspects; loss, perikaryal expansion and abnormal arrangement of neurons, are independent at least partly. Indeed, Purkinje cells are sometimes depleted after long-term administration of anticonvulsant such as diphenylhydantoin [9, 30]. It is then possible that this depletion of Purkinje cells had been influenced by the long-term administration of anticonvulsants, which also explains the robust appearance of spheroids in the gracilis nucleus (Fig. 2l).

In summary, we were successful in localizing terminal sialic acid in the lamellar structure found in a rare autopsy case of sialidosis type I carrying pathological mutations in the lysosomal sialidase gene. This morphological change in the lysosome is associated more or less with deposition of lipofuscin and neuronal loss, leading to sialidosis I phenotype. It remains to be clarified how these pathological aspects are interrelated. In addition to these pathological features, more or less shared with other storage diseases, the developmental anomalies in the cerebellum and a highly resistant nature of the lymphoma are possibly related to the abnormal metabolism of sialic acid. A variety of clinical and pathological manifestations found in this patient are potentially associated with the genetic or metabolic derangement and suggest a functional multiplicity of sialidase at different aspects of normal and pathological processes [19].

## References


1. Allegranza A, Tredici G, Marmiroli P, di Donato S, Franceschetti S, Mariani C (1989) Sialidosis type I: pathological study in an adult. Clin Neuropathol 8:266–271
2. Amano N, Yokoi S, Akagi M, Sakai M, Yagishita S, Nakata K (1983) Neuropathological findings of an autopsy case of adult beta-galactosidase and neuraminidase deficiency. Acta Neuropathol 61:283–290. doi:10.1007/BF00691999
3. Bonten E, van der Spoel A, Fornerod M, Grosveld G, d'Azzo A (1996) Characterization of human lysosomal neuraminidase defines the molecular basis of the metabolic storage disorder sialidosis. Genes Dev 10:3156–3169. doi:10.1101/gad.10.24.3156
4. Buttner B, Kannicht C, Schmidt C, Loster K, Reutter W, Lee HY, Nohring S, Horstkorte R (2002) Biochemical engineering of cell surface sialic acids stimulates axonal growth. J Neurosci 22:8869–8875
5. d'Azzo A, Andria G, Strisiuglio P, Galjaard H (2001) Galactosialidosis. In: Scriver CR, Beaudet AL, Sly SW, Valle D (eds) The metabolic and molecular bases of inherited diseases, 8th edn. McGraw-Hill, New York, pp 3811–3826
6. Durand P, Ghetti R, Cavalieri S, Borrone C, Tondeur M, Michalski JC, Strecker G (1977) Sialidosis (mucolipidosis I). Helv Paediatr Acta 32:391–400
7. Gonatas NK, Terry RD, Winkler R, Korey SR, Gomez CJ, Stein A (1963) A case of juvenile lipidosis: the significance of electron microscopic and biochemical observations of a cerebral biopsy. J Neuropathol Exp Neurol 22:557–580. doi:10.1097/00005072-196310000-00001
8. Guazzi GC, Ghetti B, Barbieri F, Cecio A (1973) Myoclonus-epilepsy with cherry-red spot in adult. Acta Neurol (Napoli) 28:542–549
9. Hofmann WW (1958) Cerebellar lesions after parenteral dilantin administration. Neurology 8:210–214
10. Itoyama Y, Goto I, Kuroiwa Y, Takeichi M, Kawabuchi M, Tanaka Y (1978) Familial juvenile neuronal strage disease. New disease or variant of juvenile lipidosis? Arch Neurol 35:792–800
11. Kato T, Wang Y, Yamaguchi K, Milner CM, Shineha R, Satomi S, Miyagi T (2001) Overexpression of lysosomal-type sialidase leads to suppression of metastasis associated with reversion of malignant phenotype in murine B16 melanoma cells. Int J Cancer 92:797–804. doi:10.1002/ijc.1268
12. Koga M, Sato T, Ikuta F, Nakashima S, Kameyama K, Kojima K (1978) An autopsy case of familial neurovisceral storage disease of late onset. Folia Psychiatr Neurol Jpn 32:299–308
13. Kristensson K, Sourander P (1966) Occurrence of lipofuscin in inherited metabolic disorders affecting the nervous system. J Neurol Neurosurg Psychiatr 29:113–118. doi:10.1136/jnnp.29.2.113
14. Lowden JA, O'Brien JS (1979) Sialidosis: a review of human neuraminidase deficiency. Am J Hum Genet 31:1–18
15. Maroteaux P, Poissonnier M, Tondeur M, Strecker G, Lemonnier M (1978) Sialidose par deficit en alpha (2–6) neuraminidase sans atteinte neurologique. Mucolipidose de type I? Arch Fr Pediatr 35:280–291
16. Milner CM, Smith SV, Carrillo MB, Taylor GL, Hollinshead M, Campbell RD (1997) Identification of a sialidase encoded in the human major histocompatibility complex. J Biol Chem 272:4549–4558. doi:10.1074/jbc.272.7.4549

17. Mitoma H, Uchihara T, Yokota T, Furukawa T, Tsukagoshi H (1993) Action myoclonus induced by visually guided movement. J Neurol 241:92–95. doi:10.1007/BF00869770
18. Miyagi T, Wada T, Yamaguchi K, Hata K (2004) Sialidase and malignancy: a minireview. Glycoconj J 20:189–198. doi:10.1023/B:GLYC.0000024250.48506.bf
19. Monti E, Preti A, Venerando B, Borsani G (2002) Recent development in mammalian sialidase molecular biology. Neurochem Res 27:649–663. doi:10.1023/A:1020276000901
20. Naganawa Y, Itoh K, Shimmoto M, Takiguchi K, Doi H, Nishizawa Y, Kobayashi T, Kamei S, Lukong KE, Pshezhetsky AV, Sakuraba H (2000) Molecular and structural studies of Japanese patients with sialidosis type 1. J Hum Genet 45:241–249. doi:10.1007/s100380070034
21. O'Brien JS (1977) Neuraminidase deficiency in the cherry red spot-myoclonus syndrome. Biochem Biophys Res Commun 79:1136–1141. doi:10.1016/0006-291X(77)91124-X
22. Oyanagi K, Ohama E, Miyashita K, Yoshino H, Miyatake T, Yamazaki M, Ikuta F (1991) Galactosialidosis: neuropathological findings in a case of the late-infantile type. Acta Neuropathol 82:331–339. doi:10.1007/BF00296543
23. Pshezhetsky AV, Richard C, Michaud L, Igdoura S, Wang S, Elsliger MA, Qu J, Leclerc D, Gravel R, Dallaire L, Potier M (1997) Cloning, expression and chromosomal mapping of human lysosomal sialidase and characterization of mutations in sialidosis. Nat Genet 15:316–320. doi:10.1038/ng0397-316
24. Rapin I, Goldfischer S, Katzman R, Engel J Jr, O'Brien JS (1978) The cherry-red spot-myoclonus syndrome. Ann Neurol 3:234–242. doi:10.1002/ana.410030309
25. Sasaki T, Akimoto Y, Sato Y, Kawakami H, Hirano H, Endo T (2002) Distribution of sialoglycoconjugates in the rat cerebellum and its change with aging. J Histochem Cytochem 50:1179–1186
26. Sawada M, Moriya S, Saito S, Shineha R, Satomi S, Yamori T, Tsuruo T, Kannagi R, Miyagi T (2002) Reduced sialidase expression in highly metastatic variants of mouse colon adenocarcinoma 26 and retardation of their metastatic ability by sialidase overexpression. Int J Cancer 97:180–185. doi:10.1002/ijc.1598
27. Spranger J, Gehler J, Cantz M (1977) Mucolipidosis I—a sialidosis. Am J Med Genet 1:21–29. doi:10.1002/ajmg.1320010104
28. Suzuki O, Nozawa Y, Kawaguchi T, Abe M (2003) Alpha-2, 6-sialylation of L-PHA reactive oligosaccharides and expression of *N*-acetylglucosaminyltransferase V in human diffuse large B cell lymphoma. Oncol Rep 10:1759–1764
29. Thomas GH (2001) Disorders of glycoprotein degradation: α-mannosidosis, β-mannosidosis, fucosidosis, and sialidosis. In: Scriver CR, Beaudet AL, Sly SW, Valle D (eds) The metabolic and molecular bases of inherited diseases, 8th edn. McGraw-Hill, New York, pp 3507–3533
30. Utterback RA, Ojeman R, Malek J (1958) Parenchymatous cerebellar degeneration with dilantin intoxication. J Neuropathol Exp Neurol 17:516–519
31. Yamano T, Shimada M, Matsuzaki K, Matsumoto Y, Yoshihara W, Okada S, Inui K, Yutaka T, Yabuuchi H (1986) Pathological study on a severe sialidosis (alpha-neuraminidase deficiency). Acta Neuropathol 71:278–284. doi:10.1007/BF00688050